Tomography Imaging of Concrete by Surface Waves

Research Institute of Technology, Tobishima Corporation, Member, Hwa Kian CHAI
Department of Materials Science and Engineering, University of Ioannina, Non-member, Dimitrios G. AGGELIS
Research Institute of Technology, Tobishima Corporation, Member, Shohei MOMOKI
College of Science and Technology, Nihon University, Member, Yoshikazu KOBAYASHI
Graduate School of Engineering, Kyoto University, Member, Tomoki SHIOTANI

1. Introduction

This study investigates the suitability of surface waves to be adopted for tomography imaging of concrete structures. Experimental program was set up to examine phase velocity change of surface waves with regard to artificial defect embedded in homogeneous concrete. Using multipoint source-receiver arrangement on one specimen surface, different sets of waveforms were excited/ collected and processed to compute phase velocities of surface waves for each ray path. Based on the reconstructed phase velocity tomograms, the locations of defect within the measured area could be identified as regions with lower phase velocity in comparison the sound concrete region.

2. Experimental

The specimen used in the experimental program was a 1500×1500×300 mm concrete slab. To model void in concrete, four 5 mm-thick circular polystyrene plates of 300 mm in diameter were installed into the specimen before casting. The polystyrene plates were located at 30 mm, 60 mm, 100 mm and 140 mm from the top of measurement surface, respectively. For stress wave measurement, Fujiceramics SAF51 accelerometers with a flat response up to approximately 30 kHz were mounted on the specimen surface to form a 4× 4 matrix arrangement, as illustrated in **Fig. 1**. The distance between two adjacent sensors was 300 mm in both the vertical and horizontal directions. In order to measure surface wave velocity of sound concrete, nine accelerometers were attached in a straight array of 150 mm spacing. Four locations of sound concrete portions were measured to compute the average. During the measurement, stress waves were generated by hitting the concrete surface with a steel ball hammer. Three different ball diameters of 5 mm, 8 mm and 15 mm were used, resulting in generating stress waves of different frequency characteristics in accordance to their respective contact time with concrete surface. A 16-channel TEAC GX-1 waveform acquisition system was used to record waveform data at an interval of 5 μs for up to 0.02 s. Each set of impact was made by continuing hitting the specimen surface with a steel ball hammer for 5 seconds, resulting in generating about 20 impacts in a set of waveforms recorded by each accelerometer. The impact was conducted near one accelerometer configured as the trigger, while the rest as receivers to record arriving waveforms. The acquisition was synchronized such that all channels would start recording at the same time once the trigger channel was excited. In the case for acquiring observed data for tomography reconstruction, the impact and recording process was repeated by subsequently setting the next accelerometer as the trigger until all accelerometers have been covered. This summed up to 240 sets of waveforms for each hammer. For measuring the surface wave velocity of sound concrete using the straight sensor array, the trigger was only configured for the outermost accelerometer in the array at one end, before shifting to the opposite end. This resulted in two sets of waveform for each array and summing up to a total of 8 data sets for the four locations of sound concrete. In both types of measurements, each set of recorded waveform was stacked accordingly to increase sound to noise ratio before further processing.

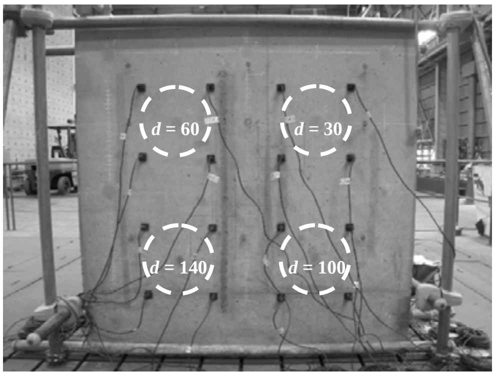

Fig.1 Specimen and arrangement of sensor (*d*: depth of polystyrene plate from measured surface in mm)

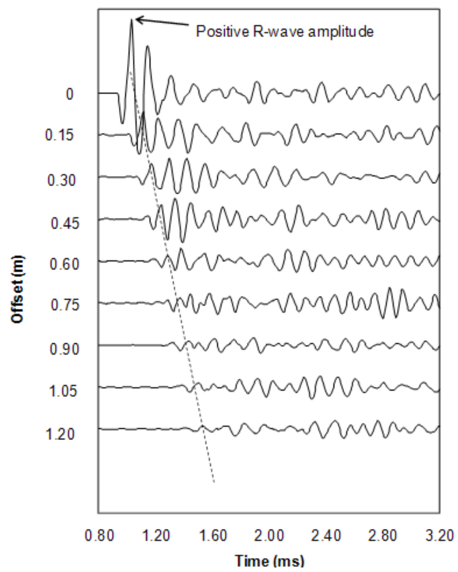

Fig. 2 Stacked time-series obtained from measuring sound concrete in a straight array

3. Results

Examples of stacked time-series data acquired from the straight line measurement of sound concrete are shown in **Fig. 2**. The peaks of arriving surface waves could be readily recognized because they have the most energy compared to the preceding amplitudes that represent body waves. For waveforms recorded by sensors that were distant from the impact source, a drawn line was extended to aid identify the surface wave amplitudes that have become much less indicative because of scattering and attenuation. The velocity of surface waves was expressed as the inverse of gradient from linear regression of time-distance plot. The average surface wave velocities by steel ball hammers of 3 mm, 8 mm and 15 mm in diameters were marked as 2255 m/s, 2218 m/s and 2236 m/s, respectively for the sound concrete. The velocity results would serve as the reference values for sound concrete and initial data for tomography reconstruction model.

Keywords: concrete, phase velocity, surface waves, tomography technique

Address: Research Institute of Technology, Tobishima Corporation, 5472 Kimagase, Noda, Chiba 270-0222 Tel: 04-7198-7559

To analyze surface waves, it was required to extract from the measured waveform information pertaining to surface waves only. This was carried out by manually processing the time-series data to retain amplitudes related to the first arriving surface waves, while "zeroing" all the preceding and subsequent amplitudes. The processing required identification of time window containing the main surface wave portion as anticipated based on the typical velocity. **Fig. 3** shows an example of the processed time series and the corresponding frequency response by fast Fourier transform (FFT). It can be noticed that the frequency response of the processed waveform has become more clear-cut, showing a peak frequency belonging to the surface wave component. Using the measured surface wave velocity and peak frequency values, the dominant wavelengths of surface waves were calculated as 110 mm, 188 mm and 240 mm for hammer diameters of 3 mm, 8 mm and 15 mm, respectively.

Fig. 4 gives typical phase velocity, V_{ph} versus frequency, f plots for both cases of surface waves propagating on the sound concrete as well as the portion embedded with defect, computed using data of hammer with ball diameter of 15 mm. It is also to be noted that the calculated dominant wavelength was greater in magnitude than the defect depth, which was located 30 mm from the measurement surface. Within the selected frequency range, it can be noticed that V_{ph} was in the range of 2250 m/s ~ 2500 m/s for the case of sound concrete. The results tallied with the ones acquired from measuring the sound concrete using a straight array. On the other hand, it was also indicated that for propagation paths containing the defect, surface wave velocity in general has decreased to less than approximately 1900 m/s. The decrease inferred that the energy of surface waves has penetrated deep enough to be distorted by the defect to result in a different behaviour of propagation. It was also noted that for most of the other measured data with defect depth greater than the dominant wavelength of surface waves, similar trend as shown in **Fig. 4** prevailed. Taking into account the size of defects, specifically their small thickness, the phase velocity decrease of approximately 500 m/s can be regarded as sensitive in manifesting the effect of an anomaly has on the behaviour of surface waves.

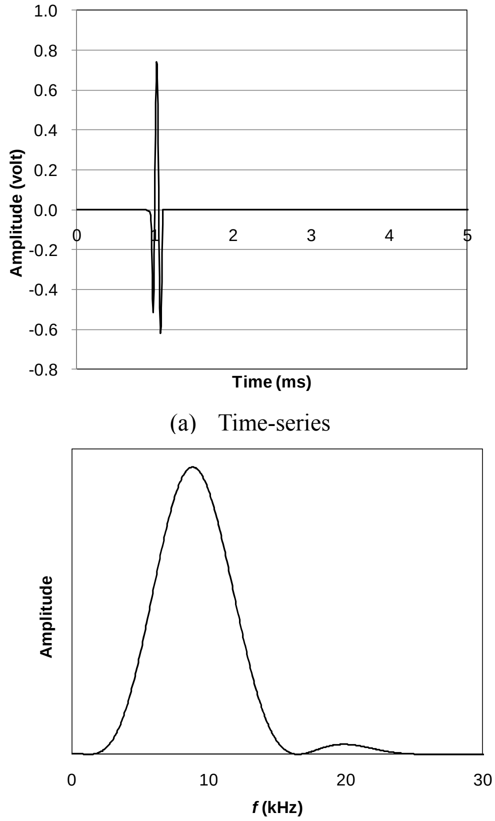

(a) Time-series

(b) Frequency response

Fig. 3 Processed waveform

For tomography reconstruction, a 6×6 square mesh of 150 mm was adopted to model the measured area. The V_{ph} values at peak frequencies corresponding to the respective hammer diameters were used as the observed data at the measured locations. The computation was carried out for 20 iterations to achieve satisfactory convergence. **Fig. 5** presents the result of tomography reconstruction using measured data by the 15 mm steel ball hammer. The result was expressed in the form of V_{ph} distribution of the measured area, indicating lower magnitudes for locations where defects could be found. Although it is to be noted that the circular shape of the defects was not accurately represented by the low velocity regions, the generated surface wave has penetrated sufficiently deep to be distorted by even the deepest defect (depth=140 mm) to cause change in propagation behaviour, which resulted in drop of phase velocity. As for the cases of 3 mm and 8 mm-steel ball hammers, which generated surface waves with shorter wavelengths compared to those by the 15 mm-steel ball hammer, less effective visualizations were found. In particular, the tomography results by both hammers did not suggest the existence of the 140 mm-deep defect.

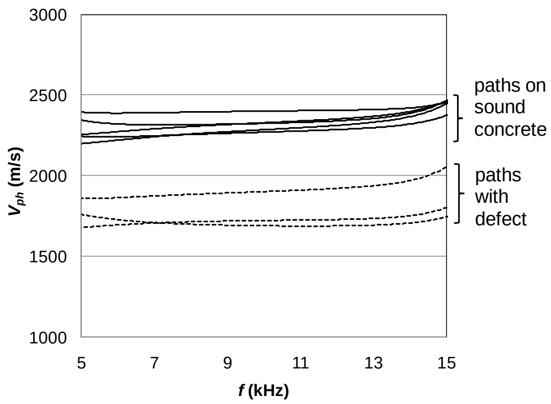

Fig. 4 Dispersion curves

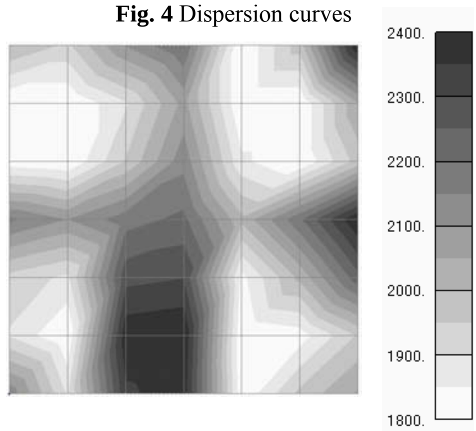

Fig. 5 Tomography reconstruction by 15 mm-steel ball hammer (unit in m/s)

4. Concluding Remark

The feasibility of surface waves for tomography imaging of concrete was investigated experimentally. To minimize the influence of reflected body waves from the free boundaries of the specimen, the acquired waveforms were pre-processed to extract the first arriving surface waves. Results showed that phase velocity of surface waves was very sensitive to the embedded defect, provided the surface waves have penetrated sufficiently deep to be distorted by the defect. Also, the distortion of surface wave energy by the defect was pronounced by the translation of the whole dispersion curve to lower values, especially for the longer wavelength excitation. Tomography results confirmed the suitability of the measurement method and data analysis procedure for visualizing this kind of subsurface defects. It was demonstrated that by increasing the dominant wavelength of surface waves, wave penetration could be improved and thus deeper defect could be detected.

Acknowledgement The support by Japan Society of the Promotion of Science under Grant-in-Aid for Young Scientists (Grant No: 20860100) is appreciated.